

How a transport problem paradigm coincides with electron-positron pair nucleation results

A. W. Beckwith

Department of Physics and Texas Center for Superconductivity and Advanced Materials at the University of Houston

Houston, Texas 77204-5005 USA

ABSTRACT

To simplify phenomenology modeling used for charge density wave (CDW) transport, we apply a wavefunctional formulation of tunneling Hamiltonians to a physical transport problem characterized by a perturbed washboard potential. To do so, we consider tunneling between states that are wavefunctionals of a scalar quantum field . **I-E** curves that match Zener curves — used to fit data experimentally with wavefunctionals congruent with the false vacuum hypothesis. This has a very strong convergence with electron-positron pair production representations. The similarities argue in favor of the new pinning gap paradigm proposed for quasi-one-dimensional metallic transport problems.

Correspondence: A. W. Beckwith: projectbeckwith2@yahoo.com.

PAC numbers: 03.75.Lm, 11.27.+d, 71.45.Lr, 75.30.Fv , 85.25.Cp

I. INTRODUCTION

As of 1985, Dr. John Miller used a Zener curve fitting polynomial to match qualitatively current vs. electric field values data he obtained from applying an electric field to a NbSe_3 crystal at low temperatures.¹ This is a first derivation of an analytical current expression that improves the Zener curve fit and has overlap with a pinning gap presentation of tunneling as an alternative to Gruner's classical model of charge density wave (CDW) transport.² This derivation permits comparison with Schwigner's³ work in the 1950s predicting the likelihood of formation of electron-positron pairs; this became a good qualitative fit once when Lin⁴ generalized Schwigner's³ results for general dimensions.

In short, we argue that a qualitatively good fit between our analytical expression and a multi-dimensional generalization of Schwigner's³ expression, which in Lin⁴ was restricted to the one-dimensional case for electron-positron pair nucleation, shows that a pinning gap interpretation of tunneling in quasi-one-dimensional systems for charge density waves (CDW) is appropriate and optimal for experimental data sets. This supports the conclusion that our analytical results improvement over the earlier Zener curve fit approximation given by Miller et al¹ was not accidental and contains serious physics worthy of consideration.

Herein, we will present a new CDW transport physics procedure for calculating current I vs. E electric field plots for quasi-one-dimensional metals, assuming:

- i. The current I is directly proportional to the modulus of the diagonal terms for the tunneling Hamiltonian. The reasons for this non-standard choice will become clear later on in the text. This tunneling Hamiltonian uses a functional integral

version of an expression used initially by Tinkham⁵ for scanning electron microscopy.

- ii. Gaussian wavefunctionals are chosen to represent the initial and final states of a soliton-anti soliton pair (S-S') traversing a pinning gap presentation of impurities in a quasi-one-dimensional metallic lattice. These wavefunctionals replace the wave functions Tinkham⁵ used in his tunneling Hamiltonian (T.H.) matrix element and are real-valued.
- iii. The pinning gap means that a washboard potential with small driving term⁶ $\mu_E \cdot (\phi - \Theta)^2$ added to the main potential term of the washboard potential, is used to model transport phenomenology. We also argue that this potential permits domain wall modeling of S-S' pairs.⁷ In this situation, μ_E is proportional to the electrostatic energy between the S-S' pair constituents (assuming a parallel plate capacitor analogy); Θ is a small driving force we will explain later, dependent upon a ratio of an applied electric field over a threshold field value. As we show later, the dominant washboard potential term will have the value of (pinning energy) times $(1 - \cos\phi)$

It is useful to note that Kazumi Maki,⁹ in 1977, gave the first generalization of Sidney Coleman's least action arguments⁸ to NbSe_3 electrodynamics. We use much the same pinning potential, with an additional term due to capacitance approximation of energy added by the interaction of a S-S' pair with each other.⁶ While Dr. Maki's work is very complete, it does not include in a feature we found of paramount importance, that of the effects of a threshold electric field value to 'turn on' effective initiation of S-S' pair transport across a pinning gap. It is also relevant to note that we previously found¹⁰ that a

topological soliton style arguments can explain why the potential lead to the least action integrand collapsed to primarily a quadratic potential contribution, which permits treating the wavefunctional as a Gaussian. As would be expected, the ratio of the coefficient of pinning gap energy of the Washboard potential used in NbSe_3 modeling to the quadratic term $\mu_E \cdot (\phi - \Theta)^2$ used in modeling energy stored in between S-S' pairs was fixed by experiment to be nearly 100 to 1, which is a datum we used in our calculations.¹¹

In several dimensions, we find that the Gaussian wavefunctionals would be given in the form given by Lu.¹² The analytical result we are working with is a one-dimensional version of a ground-state wavefunctional of the form¹²

$$|0\rangle^o = N \cdot \exp \left\{ - \int_{x,y} (\phi_x - \varphi) \cdot f_{xy} \cdot (\phi_y - \varphi) \right\} \quad (1)$$

This is for a non-perturbed, core Hamiltonian in several dimensions of the form

$$H_o = \int_x \left[\frac{1}{2} \cdot \Pi_x^2 + \frac{1}{2} \cdot (\partial_x \phi_x)^2 + \frac{1}{2} \cdot \mu^2 \cdot (\phi_x - \varphi)^2 - \frac{1}{2} \cdot I_0(\mu) \right] \quad (1a)$$

we may obtain a ‘ground state’ wave functional of the form given in Eq. (1). We assume that we have¹² a robust Gaussian. So to get our Gaussian, we set

$$\frac{\partial^2 \cdot V_E}{\partial \cdot \phi^a \cdot \partial \cdot \phi^b} \propto f_{xy} \quad (2)$$

Here, we call V_E a (Euclidian-time style) potential, with subscripts a and b referring to dimensionality; and ϕ_x an ‘x dimension contribution’ of alternations of ‘average’ phase φ , as well as ϕ_y an ‘y dimension contribution’ of alternations of ‘average’ phase

φ . For the one-dimensional treatment, φ_x and φ_y are assumed to have the same value, leading to a square integrand contribution of phase.

Due to higher order terms in a perturbing potential H_1 , this becomes equivalent to a coupling-term between the different branches of this physical system. We restrict the analysis to quasi-one-dimensional cases in which we would be able to observe a ground-state looking like^{13,14}

$$\Psi \equiv c \cdot \exp(-\alpha \cdot \int dx [\phi - \phi_c]^2) \quad (3)$$

Making this step from Eq. (1) to Eq. (3) involves recognizing, when we go to one-dimension, that we look at a washboard potential with pinning energy contribution from $D \cdot \omega_p^2$ in one-dimensional CDW systems

$$\frac{1}{2} \cdot D \cdot \omega_p^2 \cdot (1 - \cos \phi) \approx \frac{-1}{2} \cdot D \cdot \omega_p^2 \cdot \left(\frac{\phi^2}{2} + \frac{\phi^4}{24} \right) \quad (3a)$$

The fourth-order phase term is relatively small, so we look instead at contributions from the quadratic term and treat the fourth order term as a small perturbing contribution to get our one dimensional CDW potential, for lowest order, to roughly look like Eq. (1a). In addition, we should note that the c is due to an error functional-norming procedure, discussed below; α is proportional to one over the length of distance between the constituent components of a S-S' pair; the phase value, ϕ_c , is set to represent a configuration of phase in which the system evolves to/from in the course of the S-S' pair evolution. This leads to^{13,14}

$$c_1 \cdot \exp\left(-\alpha_1 \cdot \int d\tilde{x} [\phi_F]^2\right) \equiv \Psi_{initial} \quad (3b)$$

As well as

$$c_2 \cdot \exp\left(-\alpha_2 \cdot \int d\tilde{x} [\phi_T]^2\right) \equiv \Psi_{final} \quad (3c)$$

In the model, we made the assumption that $(\alpha_1 \equiv \alpha_2) \equiv \alpha$; this considerably simplified the calculation of the tunneling Hamiltonian diagonal terms. We do this assuming that the values of ϕ_F, ϕ_T are the false/true vacuum phase values of the modified perturbed Washboard potential, which we represent as

[place figure 1 about here]

We find that this construction of a current qualitatively matches with Lin's⁴ generalization of Schwinger's³ electron-positron nucleation and argues in favor of a tunneling Hamiltonian construction for transport problems in quasi-one-dimensional condensed matter problems with weakly coupled scalar fields.^{13,14}

II. A TUNNELING HAMILTONIAN PROCEDURE

Traditional current treatments followed the Fermi golden rule for current density

$$J \propto W_{LR} = \frac{2 \cdot \pi}{\hbar} \cdot |T_{LR}|^2 \cdot \rho_R(E_R) \quad (4)$$

We note that $\rho_R(E_R)$ is a density of states value, which is usually a constant. Here, even assuming this being a constant, we use a functional integration elaboration of the tunneling Hamiltonian as given by

$$T_{mn} \equiv -\frac{\hbar^2}{2\mu} \int [\psi_0^* \nabla \psi_{mn} - \psi_{mn} \nabla \psi_0^*] \cdot dS \quad (5)$$

In the current vs. applied electric field derivation results, we identify the ψ_0 as the initial wavefunction at the left side of a barrier and ψ_{mn} as the final wavefunction at the right side of a barrier. Note that Tekman⁵ extended the tunneling Hamiltonian method to encompass more complicated geometries. We notice that when the matrix elements T_{kq} are small, we calculate the current through the barrier using linear response theory. This may be used to describe coherent Josephson-like tunneling of either Cooper pairs of electrons or boson-like particles, such as superfluid He atoms.^{13,14} In this case, the supercurrent is linear with the effective matrix element for transferring a pair of electrons or transferring a single boson, as shown rather elegantly in Feynman's derivation¹⁵ of the Josephson current-phase relation. This means a current density proportional to $|T|$ rather than $|T|^2$ since tunneling, in this case, would involve coherent transfer of individual (first-order) bosons rather than pairs of fermions.¹⁴

Note that the initial and final wavefunctional states was in conjunction with a pinning gap formulation of a variation of typical band calculation structures. Fig. 2 shows much of the layout for how a tilted band structure due to an applied electric field influenced the geometry of the perturbed Washboard potential problem in the situation represented in Fig. 2:

[place Figure 2 about here]

We consider that we will be working with a Hamiltonian of the form

$$H = \int_x \left[\frac{1}{2 \cdot D} \cdot \Pi_x^2 + \frac{1}{2} \cdot (\partial_x \phi_x)^2 + \frac{1}{2} \cdot \mu_E \cdot (\phi_x - \Theta)^2 + \frac{1}{2} \cdot D \cdot \omega_p^2 \cdot (1 - \cos \phi_x) \right] \quad (5a)$$

where the potential system leads to the phenomenology represented in Fig. 2 with what we have been calling V_E the Euclidian action version of the potential given above. In addition, the first term is the conjugate momentum. Specifically, we found that we had

$$\Pi_x \equiv D \cdot \partial_t \phi_x \text{ as canonical momentum density, } D \equiv \left(\frac{\mu \cdot h}{4 \cdot \pi \cdot v_F} \right), \text{ (where } \mu \equiv \frac{M_F}{m_{e^-}} \cong 10^3$$

is a Frohlich to electron mass ratio, and v_F is a Fermi velocity $> 10^3 \text{ cm/sec}$, and $D \cdot \omega_p^2$ as the pinning energy. In addition, we have that μ_E is electrostatic energy, which is analogous to having a S-S' pair represented by a separation L and of cross-sectional area A, which produces an internal field $E^* = (e^* / \epsilon \cdot A)$, where $e^* \cong 2 \cdot e^- \equiv$ effective charge and $\epsilon \equiv 10^8 \cdot \epsilon_0$ is a huge dielectric constant. Finally, the driving force term, $\Theta = 2 \cdot \pi \cdot \frac{E}{E^*}$, where the physics of the term given by $\int dx \cdot \mu_E \cdot (\phi - \Theta)^2$, leads to no instanton tunneling transitions if $\Theta < \pi \Leftrightarrow E < \frac{E^*}{2}$ which was the basis of a threshold field of the value $E_T = E^*/2$ due to conservation of energy considerations. Finally, it is important to note that experimental constraints as noted in the device development laboratory lead to $.01 < \mu_E / D \cdot \omega_p^2 \leq .015$, which we claim has also been shown to be necessary due to topological soliton arguments.

This pinning gap structure relates to the S-S' pair formation. This can most easily be seen in the following diagram of how the S-S' pair structure arose in the first place, as given by Fig. 3:

[place Figure 3 about here]

The tunneling Hamiltonian incorporates wavefunctionals whose Gaussian shape keeps much of the structure as represented by Fig. 3.

The wavefunctionals used in this problem have coefficients in front of the integrals of the phase evolutions for the initial and final states, which are the same. This meant setting the $\alpha \approx L^{-1}$ as inversely proportional to the distance between a S-S' pair.^{13,14} Following the false vacuum hypothesis,⁸ we have a false vacuum phase value $\phi_F \equiv <\phi>_1 \equiv \text{very small value}$, as well as having in CDW, a final true vacuum⁴ $\phi_T \equiv \phi_{2\pi} \equiv 2\cdot\pi + \epsilon^+$. This led to Gaussian wavefunctionals with a simplified structure. For experimental reasons, we need to have^{13,14} (if we set the charge equal to unity, dimensionally speaking)

$$\alpha \approx L^{-1} \equiv \Delta E_{gap} \equiv V_E(\phi_F) - V_E(\phi_T) \quad (6)$$

This is equivalent to the situation as represented by Fig. 4.

[place figure 4 about here]

This assumes we are using the following substitutions in the wavefunctionals

$$\begin{aligned} \Psi_f[\phi(\mathbf{x})]_{\phi=\phi_{cf}} &= c_f \cdot \exp \left\{ - \int d\mathbf{x} \alpha \left[\phi_{cf}(\mathbf{x}) - \phi_0(\mathbf{x}) \right]^2 \right\} \rightarrow \\ &c_2 \cdot \exp \left(- \alpha_2 \cdot \int d\tilde{x} [\phi_T]^2 \right) \equiv \Psi_{final}, \end{aligned} \quad (7)$$

and

$$\begin{aligned} \Psi_i[\phi(\mathbf{x})] \Big|_{\phi=\phi_{ci}} &= c_i \cdot \exp \left\{ -\alpha \int d\mathbf{x} [\phi_{ci}(\mathbf{x}) - \phi_0]^2 \right\} \rightarrow \\ c_1 \cdot \exp \left(-\alpha_1 \cdot \int d\tilde{x} [\phi_F]^2 \right) &\equiv \Psi_{initial}, \end{aligned} \quad (8)$$

III. EVALUATING THE TUNNELING HAMILTONIAN ITSELF TO GET A CURRENT' CALCULATION IN CDW

Our wavefunctionals plus the absolute value of the tunneling Hamiltonian in momentum space lead to, after a lengthy calculation,^{13,14} a way to predict how the modulus of diagonal tunneling matrix elements that are equivalent to current will influence an applied electric field. It was done in momentum space, among other things.

We¹⁴ assumed using a scaling of $\hbar \equiv 1$, in which the ‘current’ becomes^{13,14}

$$I \propto \tilde{C}_1 \cdot \left[\cosh \left[\sqrt{\frac{2 \cdot E}{E_T \cdot c_V}} - \sqrt{\frac{E_T \cdot c_V}{E}} \right] \right] \cdot \exp \left(-\frac{E_T \cdot c_V}{E} \right) \quad (9)$$

This is due to evaluating our tunneling matrix Hamiltonian with the momentum version of an F.T. of the thin wall approximation, which is alluded to in Fig. 2^{13,14} being set by

$$\phi(k_n) = \sqrt{\frac{2}{\pi}} \cdot \frac{\sin(k_n L/2)}{k_n} \quad (10)$$

We also assume a normalization of the form^{13,14}

$$C_i = \frac{1}{\sqrt{\int_0^{\frac{L^2}{2\pi}} \exp(-2 \cdot \{ \}_i \cdot \phi^2(k)) \cdot d\phi(k)}} \quad (11)$$

In doing this, $\{ \}_i$ refers to initial and final momentum state information of the wavefunctional integrands obtained by the conversion of our initial and final CDW

wavefunctional states to a $\varphi(k)$ ‘momentum’ basis. We evaluate for $i = 1, 2$ representing the initial and final wavefunctional states for CDW transport via the error function⁸

$$\sqrt{\frac{L^2}{2\pi}} \int_0^{\Psi_i^2} d\phi(k_n) = 1 \quad (12)$$

due to an error function behaving as¹⁶

$$\int_0^b \exp(-a \cdot x^2) dx = \frac{1}{2} \cdot \sqrt{\frac{\pi}{a}} \cdot \operatorname{erf}(b \cdot \sqrt{a}) \quad (13)$$

leading to a renormalization of the form¹⁴

$$\tilde{C}_1 \equiv \frac{C_1 \cdot C_2}{2 \cdot m_{e^-}}.$$

The current expression is a great improvement upon the phenomenological Zener current^{1,13,14} expression, where G_P is the limiting Charge Density Wave (CDW) conductance.

Fig. 5 illustrates to how the pinning gap calculation improve upon a phenomenological curve fitting result used to match experimental data

[place figure 5 about here]

The Bloch bands are tilted by an applied electric field when we have $E_{DC} \geq E_T$ leading to a S-S' pair shown in Fig. 1.^{13,14,17} The slope of the tilted band structure is

given by $e^* \cdot E$ and the separation between the S-S' pair is given by, as referred to in Fig. 2. Note that the $e^* \equiv 2 \cdot e^-$ due to the constituent components of a S-S' pair. And Fig 2 gives us the following distance, L , where Δ_s is a ‘vertical’ distance between the two band structures tilted by an applied electric field, and L is the distance between the constituent S-S' charge centers.

$$L = \left(\frac{2 \cdot \Delta_s}{e^*} \right) \cdot \frac{1}{E} \quad (15)$$

So then,⁴ we have $L \propto E^{-1}$. When we consider a Zener diagram of CDW electrons with tunneling only happening when $e^* \cdot E \cdot L > \varepsilon_G$ where e^* is the effective charge of each condensed electron and ε_G being a pinning gap energy, we find that Fig. 1 permits writing.^{13,14}

$$\frac{L}{x} \equiv \frac{L}{\bar{x}} \equiv c_v \cdot \frac{E_T}{E} \quad (16)$$

Here, c_v is a proportionality factor included to accommodate the physics of a given spatial (for a CDW chain) harmonic approximation of

$$\bar{x} = \bar{x}_0 \cdot \cos(\omega \cdot t) \Leftrightarrow m_{e^-} \cdot a = -m_{e^-} \cdot \omega^2 \cdot \bar{x} = e^- \cdot E \Leftrightarrow \bar{x} = \frac{e^- \cdot E}{m_{e^-} \omega^2}.$$

Realistically, an experimentalist¹⁴ will have to consider that $L \gg \bar{x}$, where \bar{x} is an assumed reference point an observer picks to measure where a S-S' pair is on an assumed one-dimensional chain of impurity sites.

IV. COMPARISON WITH LIN'S GENERALIZATION

In a 1999, Qiong-gui Lin⁴ proposed a general rule regarding the probability of electron-positron pair creation in $D+1$ dimensions, with D varying from one to three, leading, in the case of a pure electric field, to

$$w_E = (1 + \delta_{d3}) \cdot \frac{|e \cdot E|^{(D+1)/2}}{(2 \cdot \pi)^D} \cdot \sum_{n=1}^{\infty} \frac{1}{n^{(D+1)/2}} \cdot \exp\left(-\frac{n \cdot \pi \cdot m^2}{|e \cdot E|}\right) \quad (17)$$

When D is set equal to three, we get (after setting $e^2, m \equiv 1$)

$$wIII(E) = \frac{|E|^2}{(4 \cdot \pi^3)} \cdot \sum_{n=1}^{\infty} \frac{1}{n^2} \cdot \exp\left(-\frac{n \cdot \pi}{|E|}\right) \quad (18)$$

which, if graphed gives a comparatively flattened curve compared w.r.t. to what we get when D is set equal to one (after setting $e^2, m \equiv 1$)

$$wI(E) = \frac{|E|^1}{(2 \cdot \pi^1)} \cdot \sum_{n=1}^{\infty} \frac{1}{n^1} \cdot \exp\left(-\frac{n \cdot \pi}{|E|}\right) \equiv -\frac{|E|}{2 \cdot \pi} \cdot \ln\left[1 - \exp\left(-\frac{\pi}{E}\right)\right] \quad (19)$$

which is far more linear in behavior for an e field varying from zero to a small numerical value. We see these two graphs in Fig. 6.

[place Fig. 6 about here]

This is indicating that, as dimensionality drops, we have a steady progression toward linearity. The three-dimensional result given by Lin⁴ is merely the Swinger³ result observed in the 1950s. When I have $D = 1$ and obtain behavior very similar to the analysis completed for the S-S' current argument just presented,¹⁴ the main difference is in a threshold electric field that is cleanly represented by our graphical analysis. This is a major improvement in the prior curve fitting exercised used in 1985 to curve-fit data.¹

V. CONCLUSION

We restrict this analysis to ultra fast transitions of CDW;^{13,14} this is realistic and in sync with how the wavefunctionals used are formed in part by the fate of the false vacuum hypothesis.

Additionally, we explore the remarkable similarities between what we have presented here and Lin's⁴ expansion of Schwinger's³ physically significant work in electron-positron pair production. That is, the pinning wall interpretation of tunneling for CDW permits construction of **I-E** curves that match experimental data sets; beforehand these were merely Zener curve fitting polynomial constructions.^{13,14} Our new physics are and useful for an experimentally based understanding of transport problems in condensed matter physics. Having obtained^{13,14} the **I-E** curve similar to Lin's results⁴ gives credence to a pinning gap analysis of CDW transport,^{13,14} with the main difference lying in the new results giving a definitive threshold field effect, whereas both the Zener curve fit polynomial¹ and Lin's results⁴ are not with a specifically delineated threshold electric field. The derived result does not have the arbitrary zero value cut off specified for current values below given by Miller et al¹ in 1985 but gives this as a result of an analytical derivation.^{13,14} This assumes that in such a situation that the electric field is below a given threshold value. In doing this, the final results depend upon a wavefunctional presentation not materially different from mathematical results derived by Javir Casahoran¹⁸ to represent instanton physics. Furthermore, what is done here is a simpler treatment of transport modeling as is seen in older treatment in the literature¹⁹

The author wishes to thank Dr. John Miller for introducing this problem to him in 2000, as well as for his discussions with regards to the role bosonic states play in affecting the relative power law contribution of the magnitude of the absolute value of the

tunneling matrix elements used in the current calculations. In addition, Dr. Leiming Xie highlighted the importance of Eq. (9) as an improvement over Eq. (14), in this problems evaluation. The author claims sole credit for noticing Lin's derivation as to its relationship to Eq. (9) given in this document.

REFERENCES

¹ J.H. Miller, J. Richards, R.E. Thorne, W.G. Lyons and J.R. Tucker, *Phys. Rev. Lett.* **55**, 1006 (1985)

² G. Gruner, *Reviews of Modern Physics*, vol 60, No. 4, October 4, 1988, pp. 1129-1181

³ J. Schwinger, *Phys. Rev.* **82**, 664 (1951)

⁴ Q.-G. Lin, *J. Phys. G* **25**, 17 (1999)

⁵ E. Tekman, *Phys. Rev. B* **46**, 4938 (1992)

⁶ J. H. Miller, Jr., C. Ordonez, and E. Prodan, *Phys. Rev. Lett.* **84**, 1555 (2000)

⁷ J. H. Miller, Jr., G. Cardenas, A. Garcia-Perez, W. More, and A. W. Beckwith, *J. Phys. A: Math. Gen.* **36**, 9209 (2003)

⁹ K. Maki ; *Phys. Rev. Lett.* **39**, 46 (1977), K. Maki *Phys. Rev. B* **18**, 1641 (1978)

⁸ S. Coleman, *Phys. Rev. D* **15**, 2929 (1977)

¹⁰ A. Beckwith math-ph/0411031 : *An open question: Are topological arguments helpful in setting initial conditions for transport problems in condensed matter physics?*

¹¹ Private discussions with Dr. J.H.Miller about experimental phenomenology he observed in the device development laboratory, 1998-2000, TcSAM/ U. of Houston

¹² Wen-Fa Lu, Chul Koo Kim, Jay Hyung Lee, and Kyun Nahm, *Phys Rev. D* **64**, 025006 (2001).

¹³ A. Beckwith, arXIV math-ph/0406053 : *The tunneling Hamiltonian representation of false vacuum decay: II. Application to soliton-anti soliton pair creation*

¹⁴ A. Beckwith, PhD dissertation, 2001 (U. of Houston) 'Classical and Quantum models of Density wave Transport: A comparative study; E. Kreyszig, *Introductory*

functional analysis with Applications, Wiley, 1978, pp 102- 102; Nirmala Prakash, *Mathematical Perspectives on Theoretical physics*, Imperial College Press, 2000, p545-6, in particular 9c.77

¹⁵ R. P. Feynman, R. B. Leighton, and M. Sands, *The Feynman Lectures on Physics, Vol. III*, Addison-Wesley (1964)

⁸ *CRC Standard Mathematical Tables and Formulaeas, 30th Edition* CRC Press, (1996), pp. 498-499.

¹⁶ *CRC Standard Mathematical Tables and Formulaeas, 30th Edition* CRC Press, (1996), pp. 498-499.

¹⁷ John Bardeen, *Phys.Rev.Lett.* 45, 1978 (1980)

¹⁸ Javir Casahoran , *Comm. Math . Sci, Vol 1, No. 2*, pp 245-268.

¹⁹. For a reviews see: R. Jackiw's article in *Field Theory and Particle Physics*, O.; Eboli, M. Gomes, and A. Samtoro, Eds. (World Scientific, Singapore, 1990); F. Cooper and E. Mottola, *Phys. Rev.* D36, 3114 (1987); S.-Y. Pi and M.; Samiullah, *Phys. Rev.* D36, 3128 (1987); R. Floreanini and R. Jackiw, *Phys. Rev.* D37, 2206 (1988); D. Minic and V. P. Nair, *Int. J. Mod. Phys. A* 11, 2749.

FIGURE CAPTIONS

Fig. 1 Evolution from an initial state $\Psi_i[\phi]$ to a final state $\Psi_f[\phi]$ for a double-well potential (inset) in a 1-D model, showing a kink-antikink pair bounding the nucleated bubble of true vacuum. The shading illustrates quantum fluctuations about the initial and final optimum configurations of the field, while $\phi_0(x)$ represents an intermediate field configuration inside the tunnel barrier. The upper right corner of this figure is how the fate of the false vacuum hypothesis gives a difference in energy between false and true potential vacuum values.

Fig.2 A representation of Zener tunneling through pinning gap with band structure tilted by applied E field.

Fig 3 In this representation of soliton-antisoliton (S-S') pairs along a chain, the evolution of phase is spatially given by

$$\phi(x) = \pi [\tanh b(x-x_a) + \tanh b(x_b - x)].$$

Fig 4 This representation of the fate of the false vacuum in CDW shows a difference in energy between false and true vacuum values.

Fig.5: Experimental and theoretical predictions of current values. The dots represent a Zenier curve fitting polynomial; the blue circles are for the soliton-antisoliton (S-S') pair transport expression derived with a field theoretic version of a tunneling Hamiltonian.

Fig 6 Two curves representing probabilities of the nucleation of an electronpositron pair in a vacuum is a nearly-linear curve representing a 1+1dimensional system; the second curve is for a 3+ 1dimensional physical system is far less linear.

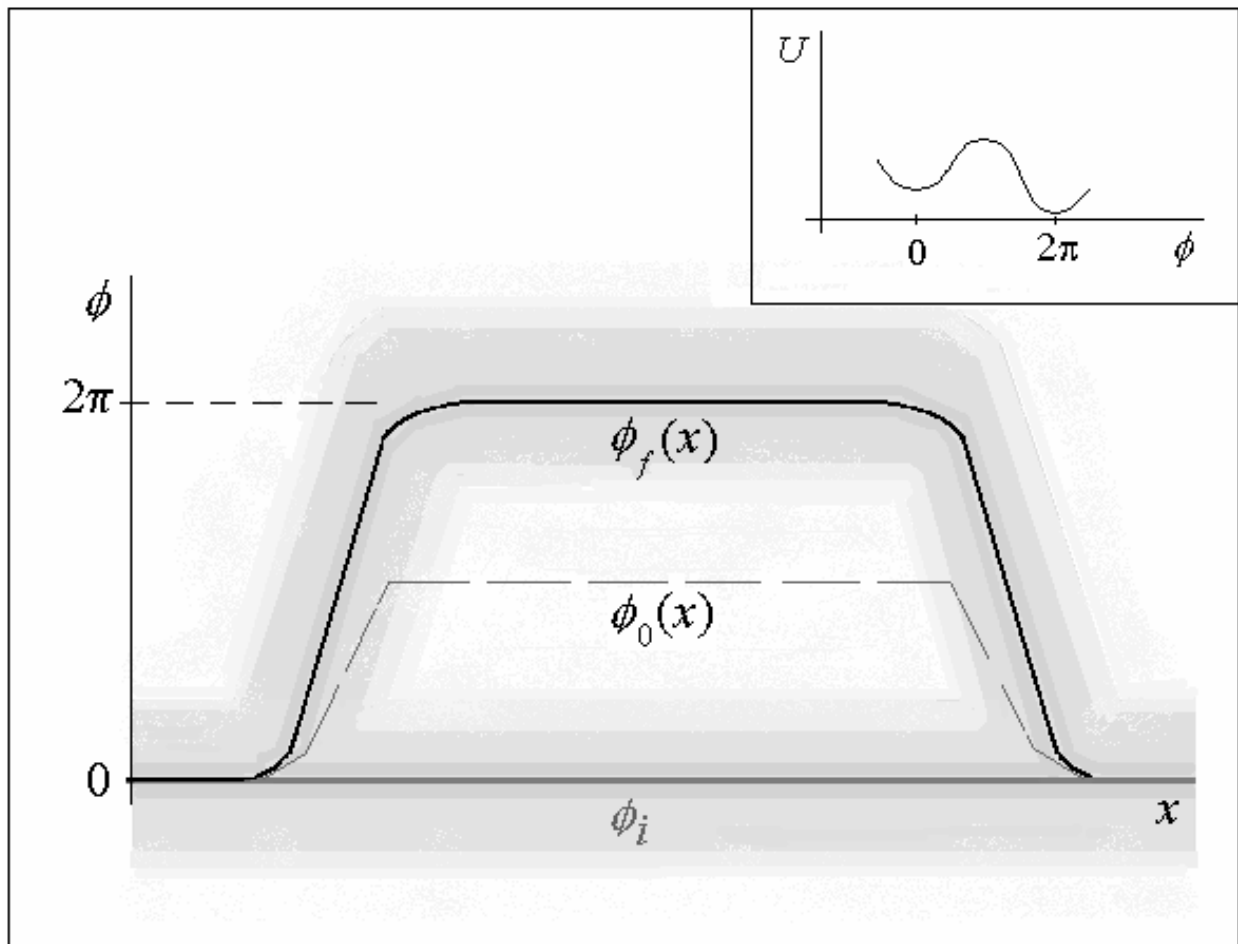


Figure 1
Beckwith

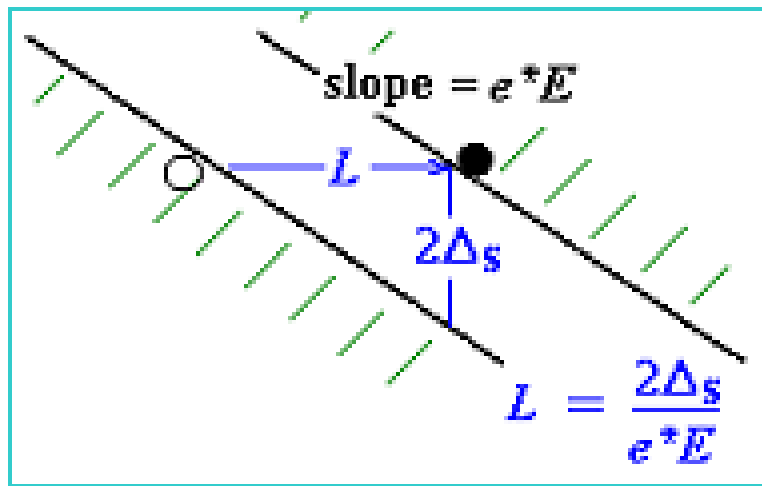


Figure 2
Beckwith

CDW and its Solitons

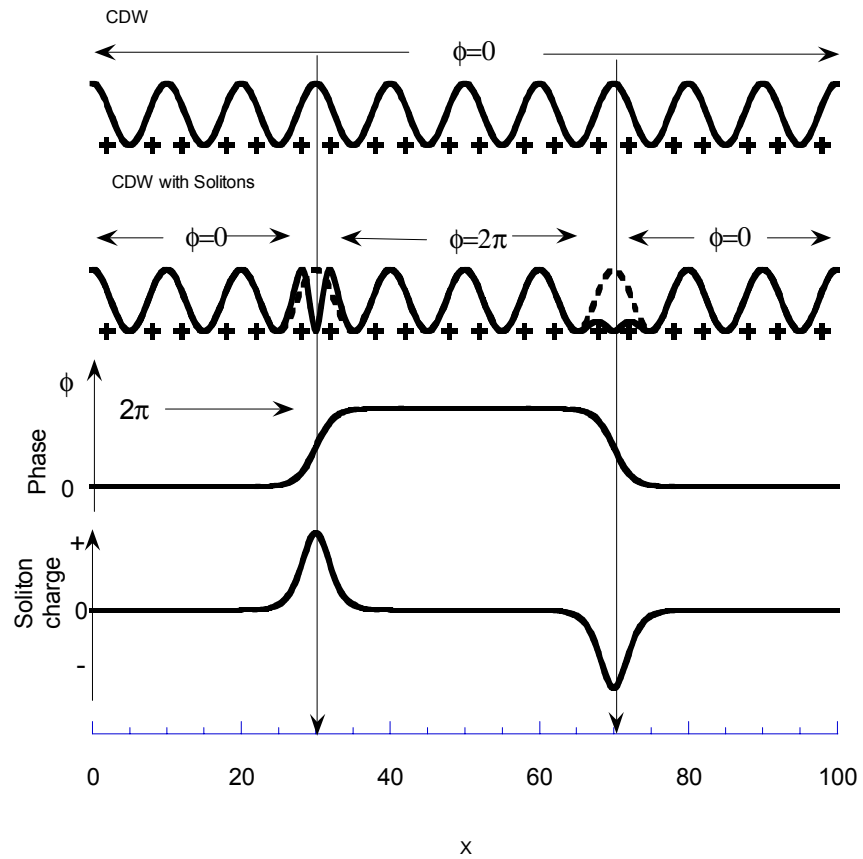


Figure 3
Beckwith

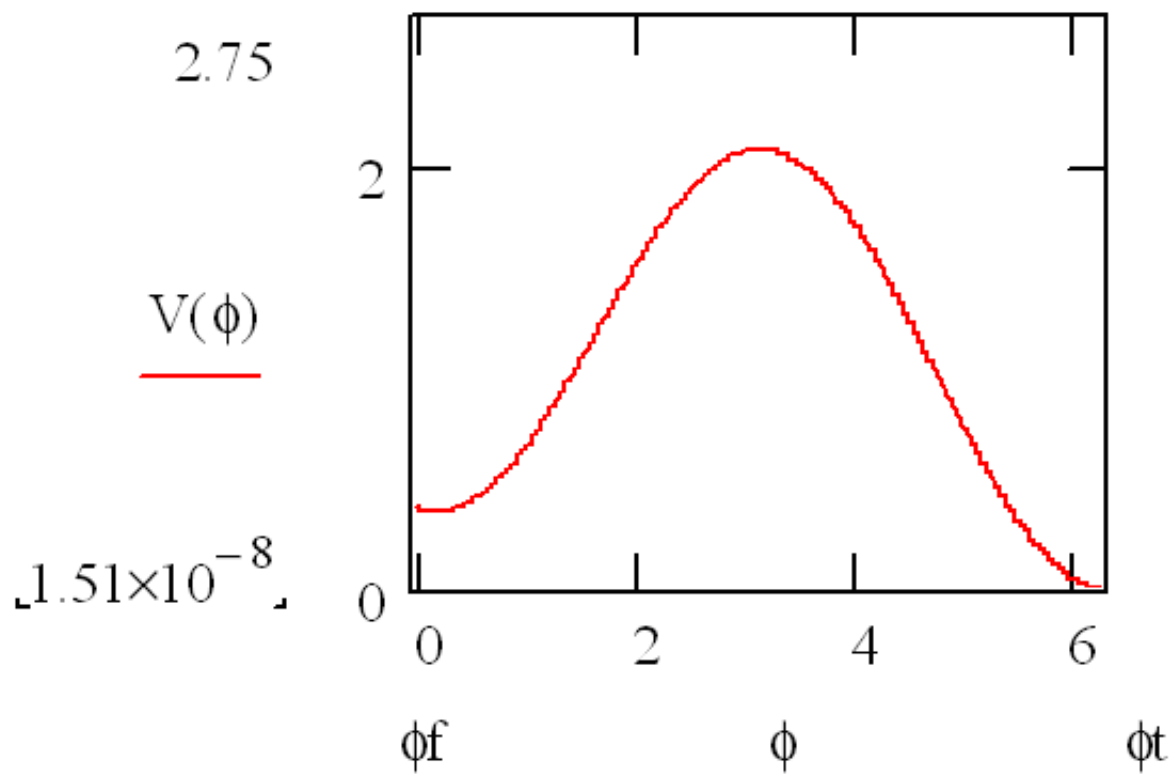


Figure 4
Beckwith

Fig 4

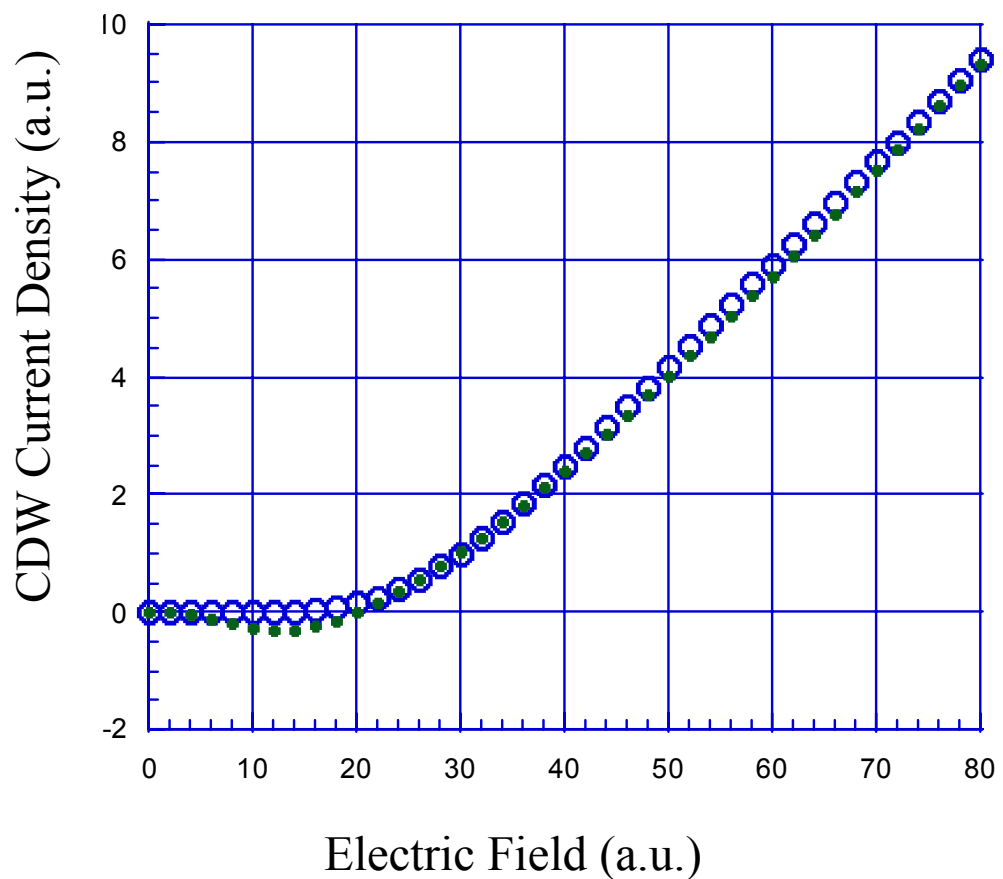


Figure 5
Beckwith

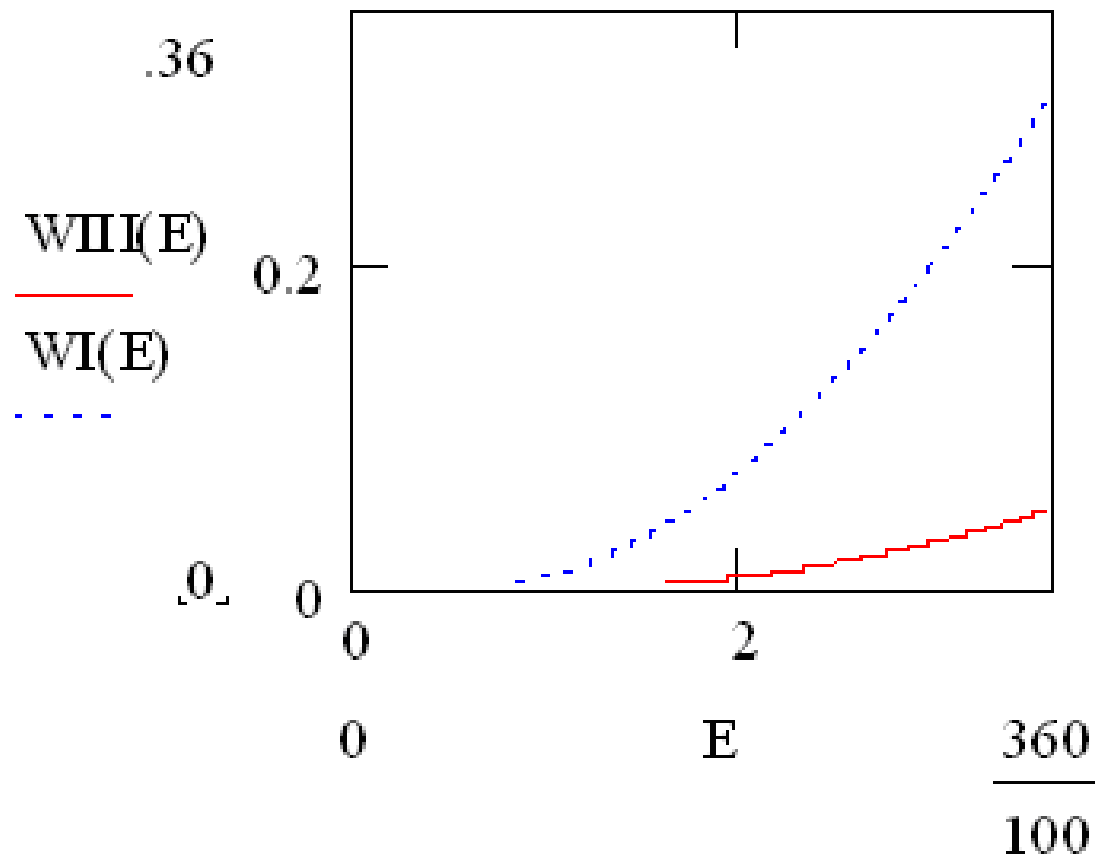


Figure 6
Beckwith